

Algebraic Decay in Hierarchical Graphs

Felipe Barra^{1, 2} and Thomas Gilbert¹

Received November 5, 2001; accepted March 23, 2002

We study the algebraic decay of the survival probability in open hierarchical graphs. We present a model of a persistent random walk on a hierarchical graph and study the spectral properties of the Frobenius–Perron operator. Using a perturbative scheme, we derive the exponent of the classical algebraic decay in terms of two parameters of the model. One parameter defines the geometrical relation between the length scales on the graph, and the other relates to the probabilities for the random walker to go from one level of the hierarchy to another. The scattering resonances of the corresponding hierarchical quantum graphs are also studied. The width distribution shows the scaling behavior $P(\Gamma) \sim 1/\Gamma$.

KEY WORDS: Survival probability; algebraic decay; Pollicott–Ruelle resonances; quantum scattering resonances.

1. INTRODUCTION

Typical Hamiltonian systems are non-integrable and have a mixed phase space, where regions of regular and chaotic motions coexist. The chaotic dynamics of mixed systems is clearly different from the fully chaotic case. This is manifest in the behavior of the survival probability in open systems.

Assume we have an infinite hierarchy of Kolmogorov–Arnold–Moser (KAM) small islands interspersed in a connected chaotic region, and suppose we draw a boundary at a given level of this hierarchy, such that the particles leaving this boundary are lost. Consider a large initial number N_0 of randomly chosen (with respect to a given probability distribution)

¹ Department of Chemical Physics, The Weizmann Institute of Science, Rehovot 76100, Israel; e-mail: thomas.gilbert@weizmann.ac.il

² Permanent address: Dept. Física, Facultad de ciencias Físicas y Matemáticas universidad de Chile, casilla 487-3 Santiago, Chile.

initial conditions in the chaotic region and let them evolve by the dynamics up to some time t . The survival probability $P(t)$ is the ratio $N(t)/N_0$ in the limit of large N_0 , where $N(t)$ is the number of particles remaining within the boundary at time t . In the typical case this probability is believed to decay algebraically,

$$P(t) \sim t^{-\delta}. \quad (1)$$

It has been argued that the algebraic decay is due to the hierarchical structure of phase space.⁽¹⁻⁶⁾ However, despite significant efforts, the mathematical understanding of the behavior described by Eq. (1) is rather poor.⁽⁷⁾ Much of our current knowledge of this problem is based on the self-similar Markov chain model,^(3,4) which provides an expression for the exponent δ in terms of the parameters of the model. Yet a precise and simple understanding of the mechanism based on dynamical properties is lacking.

In fully chaotic open systems, the survival probability decays exponentially,

$$P(t) \sim e^{-\gamma t}. \quad (2)$$

This case is well understood. The evolution operator of the probability densities, the Frobenius–Perron operator, admits a spectral decomposition in terms of Pollicott–Ruelle resonances⁽⁸⁾³ which characterize the relaxation properties. In particular, for open systems, the leading resonance is identified as the escape rate γ in Eq. (2), and describes the slowest relaxation mode of the probability distributions. We point out that in closed systems an equilibrium state exists (the leading resonance is equal to zero), and one can study the relaxation to this equilibrium state by considering the next leading resonance. In contrast, for open systems the final state does not exist due to the escape, the rate of which is characterized by the leading resonance of the Frobenius–Perron operator. We refer to ref. 10 for more details concerning the connection between open and closed systems.

The escape rate can also be interpreted as a macroscopic quantity resulting e.g., from a diffusion process described by a Fokker–Planck equation for the macroscopic density of particles. This connection between microscopic dynamics and macroscopic processes, known as the escape rate formalism,⁽⁹⁻¹³⁾ yields expressions of the transport coefficients, e.g., the diffusion coefficient, in terms of the dynamical quantities. The existence of this connection relies heavily on the hyperbolic properties of the system,

³ Note that the use of the term resonances here is restricted to the logarithms of eigenvalues of the Frobenius–Perron operator, as opposed to its use in the KAM theory, e.g., as in ref. 6.

i.e., (i) (almost) every point in phase space is assumed to be of saddle type, and (ii), for the open boundaries, the repeller is fractal.

The absence of an exponential decay rate of the survival probability for a typical system Eq. (1) is associated to anomalous transport, e.g., in a diffusive process the mean square displacement grows with a power of t not equal to 1. With this respect, the connections between macroscopic phenomena and microscopic dynamics are far less understood for typical systems than they are in the fully chaotic case.

Attempts to describe the relaxation properties of systems with mixed phase space in terms of spectral properties of the Frobenius–Perron operator have introduced regularization procedures which amount to truncating the Frobenius–Perron operator in a finite matrix representation.⁽¹⁴⁾ An alternative approach⁽¹⁵⁾ considers the presence of a vanishing noise and yields finite values of the leading relaxation rates. In both these approaches, it is worthwhile stressing that the relaxation rates are the analogues of the leading Pollicott–Ruelle resonances mentioned above in reference to relaxation in fully chaotic systems.

Our purpose in this paper is to understand what properties of the Pollicott–Ruelle spectrum characterize the algebraic as opposed to exponential decay of the survival probability. We will do so by considering a model whose finite approximations are fully chaotic, but which displays algebraic decay of the survival probability as a limiting property.

For the purpose of this endeavor, we propose to investigate the decay properties of an open one-dimensional hierarchical graph, whose survival probability turns out to decay algebraically. A graph is a collection of bonds on which a classical particle has a uniform one-dimensional motion. The bonds are interconnected by vertices where neighboring bonds meet. At the vertices, the particle undergoes a conservative collision process with the result that its velocity may change direction. In practice this collision process is determined by a random process where outputs are assigned fixed transition probabilities in terms of the inputs. A hierarchical graph is one where the lengths of the bonds and the transition probabilities obey scaling laws.⁽¹⁶⁾

The specific model we propose to study is based on a one-dimensional Lorentz lattice gas,^(17,18) the difference being that ours is a continuous time process where the separation between scatterers will be taken to satisfy a scaling law. The scattering probabilities depend on the direction of the particle, in analogy to the Lorentz lattice gas, with the further property that these probabilities change according to the index of the scatterer. Due to its connection to persistent random walks, we propose to refer to our model as a *persistent hierarchical graph*. In such a system, the evolution operator for phase space densities, the Frobenius–Perron operator, can be

written explicitly and its spectral decomposition expressed in terms of the Pollicott–Ruelle resonances s_j .⁽¹⁹⁾ This in turn yields the expression for the survival probability :

$$P(t) = \sum_{j=0}^{\infty} A_j e^{s_j t}, \quad (3)$$

where the amplitudes A_j can be expressed in terms of the eigenstates associated to the corresponding resonances. The Pollicott–Ruelle resonance spectrum is located in the lower half-plane, $\text{Re } s_j < 0$. We note that the Perron–Frobenius operator is here defined on a rigged Hilbert space, whose dimension is infinite.⁽¹⁰⁾

It is a general property that finite open graphs are fully chaotic systems. Indeed there is a gap empty of resonances, i.e., the closest resonance to the imaginary axis is real and isolated, so that it dominates the sum in Eq. (3). This resonance is the escape rate. Thus in this case the survival probability decays exponentially as in Eq. (2).

On the contrary, in the semi-infinite open hierarchical graph, because the lengths of the bonds and the transition probabilities scale in terms of some parameters (see Section 2.2), we will see that the decay of the survival probability is algebraic as in Eq. (1). Indeed the power law behavior can emerge in the limit of infinite graphs from the expression (3), because there is an accumulation of resonances going to zero and distributed with a particular density. In fact, if the amplitudes and the decay rates satisfy $A_j = \alpha \alpha^j$ and $s_j = -b \beta^j$ with α , β , a and b some real functions of the parameters of the model ($0 < \alpha, \beta < 1$), then, evaluating the sum in Eq. (3) by the steepest decent method we get the power law decay of Eq. (1) with

$$\left. \begin{array}{l} A_j = \alpha \alpha^j \\ s_j = -b \beta^j \end{array} \right\} \Rightarrow \delta = \frac{\ln \alpha}{\ln \beta} \quad (4)$$

We will show in Section 4 that indeed these scaling behaviors for the spectrum s_j and for the amplitudes A_j hold for persistent hierarchical graphs. We further point out a connection between the parameters α and β and the scaling parameters of dynamical traps:^(20, 21) α is the spatial scaling parameter and $1/\beta$ the temporal one. We will come back to this in the conclusions.

As already mentioned, every finite size approximation of a persistent hierarchical graph is a fully chaotic system. This provides means of making further comparisons between typical and fully chaotic systems. Dynamical quantities, such as the topological pressure (henceforth referred to as free energy) will be considered.

Recent studies consider the question how the hierarchical structure and the dynamics of a typical Hamiltonian system shows up in quantum

properties. It was shown by a semi-classical argument⁽²²⁾ that Eq. (1) leads to fractal conductance fluctuations on an energy scale larger than the mean level spacing. These fractal conductance fluctuations are decorated with peaks corresponding to isolated resonances at a small energy scale,⁽¹⁶⁾ which are associated to “hierarchical” states and are distributed according to $p(\Gamma) \sim 1/\Gamma$, with Γ the width of the scattering resonance in the wave-number plane, to be defined in Section 6.

Quantum properties of graphs are not without their own interest. Spectral properties of closed quantum graphs have been considered in ref. 23 where quantum graphs were introduced for the first time as a model for quantum chaos. Other spectral properties were considered in refs. 24–26. Dynamics,⁽²⁷⁾ scattering⁽²⁸⁾ and localization in infinite disordered graphs⁽²⁹⁾ have also been considered. On the other hand the classical dynamics has been studied in detail in ref. 30. Here we will also study properties of the scattering resonances in a quantum realization of the persistent hierarchical graph.

The plan of the paper is as follows. In Section 2 we discuss general properties of classical and quantum graphs and introduce the persistent hierarchical graphs in some detail. The survival probability is defined in Section 3, where we give its expression in terms of the spectral decomposition of the evolution operator. Section 4 presents the calculation of the spectrum of the persistent hierarchical graph. Some properties of the free energy are studied in Section 5. In Section 6 we turn to the quantum description of persistent hierarchical graphs and, in particular, analyze the spectrum of scattering resonances. Finally conclusions and perspectives are drawn in Section 7.

2. HIERARCHICAL GRAPHS AND OUR MODEL

2.1. General Survey

A graph is a collection of B one-dimensional bonds, connected by vertices, where a particle moves freely. The position of the particle on the graph is described by a coordinate x_b . The index b refers to a particular bond and x_b to the position on that bond, with $0 < x_b < l_b$, where l_b denotes the length of the corresponding bond. Here we consider oriented graphs where bonds have directions. Thus to each “physical” bond corresponds two oriented bonds, and therefore the number of oriented bonds is $2B$.

In a quantum graph the dynamics of the particle on a bond is governed by the free Schrödinger equation. When the particle arrives to a vertex, a scattering process determines the *probability amplitude* $\sigma_{bb'}$ for being reflected or transmitted to the other connected bonds.

These systems admit a classical limit which corresponds to a particle moving at constant velocity on the bonds and undergoing a conservative scattering process at the vertices (the classical limit of the quantum scattering process), determined by the *probabilities* $P_{bb'} = |\sigma_{bb'}|^2$ of being reflected or transmitted to other bonds. The classical dynamics is Markovian, i.e., there is no memory effect.

Open or *scattering* graphs, have some infinite leads c , from where a particle can escape and never return.

Hierarchical graphs are a particular class of graphs consisting of a self-similar collection of unit cells, which are topologically identical and whose characteristic lengths follow a given scaling law. In the classical case, the transition probabilities are taken to satisfy a scaling property, such as in a continuous self-similar Markov chain.⁽³⁾ A possible example is given by a random walk on a fractal support, such as the Sierpinsky gasket, where scattering probabilities change according to the level (with respect to the fractal structure) of the vertices. A simple such example is the persistent hierarchical graph we introduce below. Other examples are the quantum version of the chain model,⁽¹⁶⁾ or the Cayley tree for quantum conduction.⁽³¹⁻³³⁾

2.2. Persistent Hierarchical Graph

The hierarchical graph that we consider is a semi-infinite one-dimensional lattice where the lengths of the bonds decay exponentially with the bond index. On this lattice, a random walker moves on the bonds with constant speed, so that the time between collisions becomes exponentially shorter as the walker moves deeper into the lattice. Moreover, at each vertex, the walker undergoes a random collision which reverses its direction with some probability q_n , which depends on the index n of the scattering vertex, or keeps the direction of the walker unchanged with probability p_n . We will label by n the (non-directed) bond between vertices n and $n+1$. A directed bond b is either $(n, +)$ or $(n, -)$. In terms of those, the following transitions $P_{bb'}$ of going from b' to b are possible :

$$b' = (n, +) \rightarrow \begin{cases} b = (n+1, +), & \text{with probability } P_{(n+1, +), (n, +)} = p_{n+1}, \\ b = (n, -), & \text{with probability } P_{(n, -), (n, +)} = q_{n+1}. \end{cases} \quad (5)$$

$$b' = (n, -) \rightarrow \begin{cases} b = (n-1, -), & \text{with probability } P_{(n-1, -), (n, -)} = p_n, \\ b = (n, +), & \text{with probability } P_{(n, +), (n, -)} = q_n. \end{cases} \quad (6)$$

All the other probabilities are zero.

The probabilities p_n and q_n are chosen so as to favor backscattering of particles as they move deeper into the lattice,

$$\begin{aligned} p_n &= p_0 \varepsilon^n, \\ q_n &= 1 - p_n, \end{aligned} \quad (7)$$

where $0 < \varepsilon < 1$ is a fixed parameter.

We study this infinite hierarchical graph by considering finite approximations made of $N + 1$ vertices with open boundary conditions at both ends. That is, infinite leads are connected to vertices 1 and $N + 1$ respectively from the left and right. For the length of the bonds l_n we assume

$$l_n = l_0 \mu^n, \quad 1 \leq n \leq N, \quad (8)$$

where l_0 is an arbitrary length scale, which we will set to one, and μ , $0 < \mu < 1$, is a (dimensionless) fixed parameter. We note that the total length of the lattice is $L_N = l_0 \mu (1 - \mu^{N+1}) / (1 - \mu)$, which is bounded by $l_0 \mu / (1 - \mu)$. A schematic representation of the system is presented in Fig. 1.

Since the particles move with constant speed, in the limit where $N \rightarrow \infty$ the particles will undergo exponentially more frequent collisions as they move to the right-most end of the lattice, and will be backscattered with exponentially increasing probability, hence, in practice, never reaching the right boundary. The escape is thus expected to be essentially due to exit from the left boundary for large enough N . Figure 2 shows the results of a numerical simulation where the number of surviving particles is plotted vs. time. The power decay is apparent at long times, with an asymptotic exponent whose value agrees within a few percents with the value to be derived in Eq. (38). The configuration of the particles surviving after that time is displayed in Fig. 3. We note that the bonds are more or less equally populated at the exception of the left-most bonds, which are unpopulated.

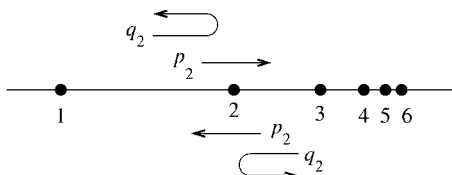


Fig. 1. Schematic illustration of the possible transitions and their probabilities for a particle colliding with a scatterer. The parameter μ is here taken to be $1/2$. There are a total of 5 bonds and 2 scattering leads in this example.

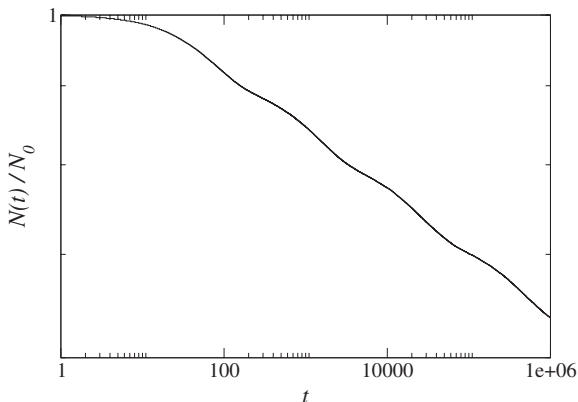


Fig. 2. Fraction $N(t)/N_0$ of particles remaining in the system after time t . The system has 25 bonds and $N_0 = 100,000$ particles are initially distributed at random positions (i.e., evenly with respect to the position on the line). The parameter values are $\varepsilon = 1/20$ and $\mu = 9/10$. Each particle is run for a maximal time 10^6 and escape times are recorded, which yields the fraction of surviving particles vs. time.

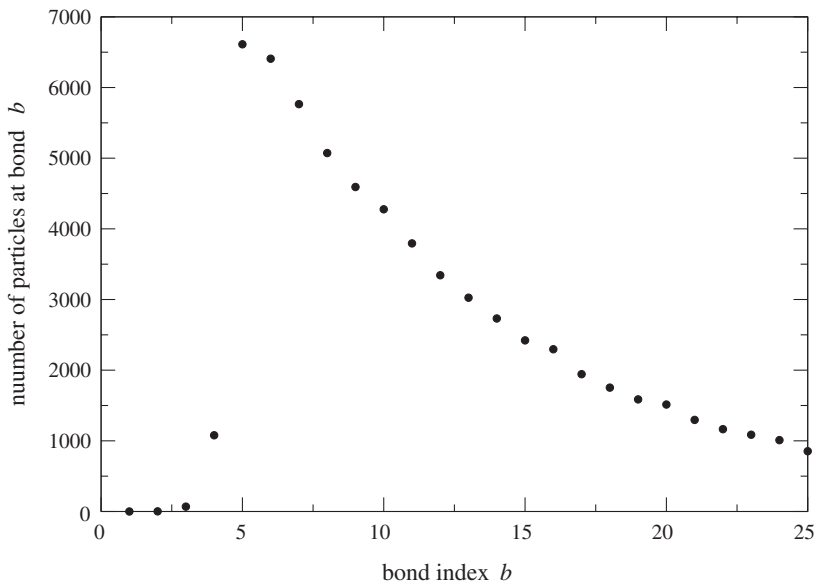


Fig. 3. Configuration of the fraction of particles surviving after $t = 10^6$ unit times. About $2/3$ of the initial number of particles have escaped after the time considered. The particles distributed on the bounds with larger indices have essentially retained their initial positions. The escape occurred from bound 1 only.

As discussed above Eq. (1), the average (with respect to random initial conditions) of the ratio of the number of particles surviving after a time t to their initial number N_0 defines the survival probability, which we would like to characterize in terms of the two parameters of the persistent hierarchical graph, namely ε and μ .

3. THE SURVIVAL PROBABILITY

The statistical average of a physical observable $A(x_b)$ defined on the bonds of the graph is given by ref. 30

$$\langle A \rangle_t = \sum_{b=1}^{2B} \frac{1}{l_b} \int_0^{l_b} A(x_b) \rho(x_b, t) dx_b = \langle A | \hat{P}^t \rho_0 \rangle, \quad (9)$$

where ρ_0 denotes the initial probability density which evolves with the Frobenius–Perron operator \hat{P}^t to give, at time t , a density $\rho(x_b, t)$ at position x_b on the bond b .

In particular, if we consider the observable $A(x_b) = l_b$ for the bonds that compose the finite part of the graph and $A(x_c) = 0$, for c a scattering lead, Eq. (9) defines the *survival probability*, i.e., the probability of finding the particle in the interior of the system at a given time t ,

$$P(t) = \sum_b \int_0^{l_b} \rho(x_b, t) dx_b. \quad (10)$$

We will henceforth reserve the notation A for this observable. One of our goals will be to show that this definition can indeed be decomposed as in Eq. (3).

Since we are interested in the time evolution at long times, we may consider the spectral decomposition of \hat{P}^t to get an asymptotic expansion valid for $t \rightarrow +\infty$ of the form

$$P(t) = \langle A | \hat{P}^t \rho_0 \rangle = \sum_j \langle A | \Psi_j \rangle e^{s_j t} \langle \tilde{\Psi}_j | \rho_0 \rangle + \dots \quad (11)$$

as a sum of exponential functions.⁴ Therefore Eq. (3) is obtained with

$$A_j = \langle A | \Psi_j \rangle \langle \tilde{\Psi}_j | \rho_0 \rangle. \quad (12)$$

⁴ Possible extra terms such as powers of the time multiplied by exponentials, $t^m \exp(s_j t)$, are not generic and may appear for particular values of the parameters of the system. See ref. 30 for a discussion of this point.

The spectral decomposition used in Eq. (11) is fully determined by the solutions of the problem⁽³⁰⁾

$$\mathbf{Q}(s_j) \chi_j = \chi_j, \quad (13)$$

which determine the Pollicott–Ruelle resonances s_j and the corresponding eigenstates χ_j . \mathbf{Q} is a $2B \times 2B$ matrix with elements given by $Q_{bb'}(s) = P_{bb'} e^{-sl_{b'}}$.

Explicit expressions for the scalar products in Eq. (12) were found in ref. 30. For the right eigenstates,

$$\langle A | \Psi_j \rangle = \sum_b \chi_j[b] \frac{1}{l_b} \int_0^{l_b} e^{-s_j \frac{x_b}{v}} A(x_b) dx_b, \quad (14)$$

and for the left eigenstates,

$$\langle \tilde{\Psi}_j | \rho_0 \rangle = \frac{1}{\sum_{b''} l_{b''} \tilde{\chi}_j[b'']^* \chi_j[b'']} \sum_b \tilde{\chi}_j[b']^* \int_0^{l_{b'}} e^{s_j \frac{x_{b'}}{v}} \rho_0(x_{b'}) dx_{b'}. \quad (15)$$

Here $\chi_j[b]$ denotes the b component of the eigenstate χ_j and $\tilde{\chi}_j^*$ denotes the complex conjugate of the left eigenvector of $\mathbf{Q}(s_j)$.

If for the initial density we take $\rho_0(x_b) = 1$, for all bonds b , and $\rho_0(x_c) = 0$ for infinite leads c , that is a uniform distribution over the finite part of the graph, we have

$$A_j = \frac{1}{s_j^2} \frac{\sum_{b,b'} l_b \chi_j(b) \tilde{\chi}_j^*(b') [e^{s_j l_{b'}} + e^{-s_j l_b} - e^{s_j(l_{b'} - l_b)} - 1]}{\sum_b l_b \chi_j(b) \tilde{\chi}_j^*(b)}. \quad (16)$$

As we will show in Section 4, the Pollicott–Ruelle resonances s_j are small so that we can expand the exponential terms in Eq. (16) and get, to first order,

$$A_j = \frac{\sum_b l_b \chi_j[b] \sum_b l_b \tilde{\chi}_j^*[b]}{\sum_b l_b \chi_j[b] \tilde{\chi}_j^*[b]}. \quad (17)$$

4. POLLICOTT–RUELLE RESONANCES

According to Eq. (13), the Pollicott–Ruelle resonances s_j are the roots of the following determinant,

$$\det[1 - \mathbf{Q}(s)] = 0. \quad (18)$$

In order to write explicitly the matrix \mathbf{Q} , we will order the states according to

$$(1, + \ 1, - \ 2, + \ 2, - \ \dots \ N, + \ N, -). \tag{19}$$

This way \mathbf{Q} has the expression

$$\mathbf{Q}(s) = \begin{pmatrix} 0 & q_1 e^{-s l_1} & 0 & 0 & 0 & \dots & 0 & 0 \\ q_2 e^{-s l_1} & 0 & 0 & p_2 e^{-s l_2} & 0 & \dots & 0 & 0 \\ p_2 e^{-s l_1} & 0 & 0 & q_2 e^{-s l_2} & 0 & \dots & 0 & 0 \\ 0 & 0 & q_3 e^{-s l_2} & 0 & 0 & \dots & 0 & 0 \\ 0 & 0 & p_3 e^{-s l_2} & 0 & 0 & \dots & 0 & 0 \\ \vdots & \vdots & \vdots & \vdots & \vdots & \ddots & \vdots & \vdots \\ 0 & 0 & 0 & 0 & 0 & \dots & q_{N+1} e^{-s l_N} & 0 \end{pmatrix}. \tag{20}$$

Since this is a sparse matrix, it is rather straightforward to compute the determinant Eq. (18),

$$\det [1 - \mathbf{Q}(s)] = \prod_{i=1}^N \delta_i, \tag{21}$$

where

$$\delta_i = 1 - q_i q_{i+1} e^{-2s l_i} \left[1 + \left(\frac{p_i}{q_i} \right)^2 \left(\frac{1}{\delta_{i-1}} - 1 \right) \right], \quad i \geq 2, \tag{22}$$

$$\delta_1 = 1 - q_1 q_2 e^{-2s l_1}. \tag{23}$$

Owing to the product structure of Eq. (21), the zeros of Eq. (18) are the zeros of δ_N . One can compute them numerically for any value of the parameters ε and μ . It should be emphasized that the identification of zeros in Eqs. (21)–(23) holds only for finite N . However, the numerical resolution of Eqs. (22)–(23) is limited to small N and, for the sake of proving Eq. (4), a perturbative approach allows an analytic treatment. This is done in what follows.

4.1. Perturbation Theory

In order to set up a perturbation scheme, we choose ε as our small parameter and note that the “unperturbed” system, $\varepsilon = 0$, corresponds to

the union of N non-interacting bonds. That is, the particles are oscillating back and forth on the same bond. The spectrum of this unperturbed system is the union of the $s_{n,m} = i \frac{m\pi}{T_n}$, $m \in \mathbb{Z}$, $n = 1, \dots, N$. The resonances with $s \neq 0$ are not degenerate and remain isolated under the perturbation, even in the limit $N \rightarrow \infty$. After the perturbation, each isolated resonance adds one contribution to Eq. (11), with an s_j whose real part is negative and $\mathcal{O}(\epsilon)$. Therefore the states associated to them decay exponentially fast (with an oscillation on top). On the other hand, the resonance $s = 0$ is the only degenerate unperturbed resonance, with a multiplicity N . As it will turn out, the perturbation acting on this resonance reduces the degeneracy by one unit at each order of the perturbation, the splitting being proportional to ϵ^j with j the order of the perturbation. Thus, in the limit $N \rightarrow \infty$, the spectrum has an accumulation point at $s = 0$. Therefore these states cannot be considered isolated and their contribution to Eq. (11) must be accounted for separately from that of the isolated resonances because it becomes an integral in this limit. This integral accounts for the algebraic decay of the surviving probability in the long time limit.

Let us discard the isolated resonances and consider only the resonances $s_{n,0}$. The eigenstates associated to the unperturbed system are solutions of the equation

$$\mathbf{Q}^{(0)}(0) \chi_n^{(0)} = \chi_n^{(0)}, \quad (24)$$

where $\mathbf{Q}^{(0)}$ is given by Eq. (20), in which ϵ is set to zero. Explicit expressions for the eigenvectors are:

$$\chi_1^{(0)} = \frac{1}{\sqrt{2}} \begin{pmatrix} 1 \\ 1 \\ 0 \\ 0 \\ 0 \\ \vdots \\ 0 \end{pmatrix}, \quad \chi_2^{(0)} = \frac{1}{\sqrt{2}} \begin{pmatrix} 0 \\ 0 \\ 1 \\ 1 \\ 0 \\ 0 \\ \vdots \\ 0 \end{pmatrix}, \dots, \quad \chi_N^{(0)} = \frac{1}{\sqrt{2}} \begin{pmatrix} 0 \\ 0 \\ \vdots \\ 0 \\ 0 \\ 1 \\ 1 \end{pmatrix}. \quad (25)$$

In order to implement the perturbation theory in powers of ϵ , we first consider the right eigenvectors. The calculation transposes straightforwardly to the case of left eigenvectors. The perturbation theory closely

resembles the standard perturbation theory for degenerate eigenvalues.⁽³⁴⁾ Let us consider linear combinations

$$\chi = \sum_{i=1}^N c_i \chi_i^{(0)}, \tag{26}$$

where the coefficients c_i are polynomials in ε , and seek approximate solutions of the system

$$\mathbf{Q}(s) \chi = \chi, \tag{27}$$

where s is a polynomial in ε and \mathbf{Q} will be expanded to a given order in ε . Writing $\mathbf{Q} = \mathbf{Q}^{(0)} + \delta\mathbf{Q}$, we substitute Eq. (26) into Eq. (27). Multiplying both sides of Eq. (27) by $\chi_i^{(0)}$, $i = 1, \dots, N$, and using Eq. (24), we obtain a system of N linear equations for the coefficients c_i , $\sum_{j=1}^N V_{i,j}(s) c_j = 0$, where $V_{i,j}(s) = \chi_i^{(0)\top} [\mathbf{Q}(s) - \mathbf{Q}^{(0)}(0)] \chi_j^{(0)}$ are the matrix elements of the perturbation operator

$$V_1(s) = \frac{1}{2} \begin{pmatrix} -2 + e^{-sI_1}(q_1 + q_2) & e^{-sI_2} p_2 & 0 & \dots & 0 \\ e^{-sI_1} p_2 & -2 + e^{-sI_2}(q_2 + q_3) & e^{-sI_3} p_3 & \dots & 0 \\ 0 & e^{-sI_2} p_3 & -2 + e^{-sI_3}(q_3 + q_4) & \dots & 0 \\ \vdots & \vdots & \vdots & \ddots & \vdots \\ 0 & 0 & 0 & \dots & -2 + e^{-sI_N}(q_N + q_{N+1}) \end{pmatrix} \tag{28}$$

The values of s are found by solving the secular equation

$$\det[V_1(s)] = 0 \tag{29}$$

to the desired power in ε .

Expanding p_n and q_n in powers of ε , we can compute the corrections to the unperturbed solution. In fact, expanding Eq. (29) up to $\mathcal{O}(\varepsilon)$ we find that only one eigenstate, $s_{1,0}$, has negative real part,

$$s_{1,0} = -\frac{p_0 \varepsilon}{2I_1} + \mathcal{O}(\varepsilon^2), \tag{30}$$

while up to this order, the others remain degenerate,

$$s_{n,0} = \mathcal{O}(\varepsilon^2), \quad n \geq 2. \tag{31}$$

The eigenvector corresponding to $s_{1,0}$ is

$$\chi(s_1) = \chi_1^{(0)} + \mathcal{O}(\varepsilon). \quad (32)$$

Hence the degeneracy remains to be lifted among the $N-1$ remaining eigenmodes. We study now how the second order correction affects the degenerate state. We proceed in a similar manner as we did for the first order. The only difference is that now $\chi_1^{(0)}$ does not belong to the base of the degenerate subspace. Accordingly the perturbation operator in this subspace is represented by the matrix $V_2 = (V_{i,j})_{2 \leq i, j \leq N}$, which is obtained from the matrix V_1 by removing the first line and first column. Expanding the equation $\det[V_2] = 0$ up to $\mathcal{O}(\varepsilon^2)$, we get a result similar to Eqs. (30)–(32) with $s_{2,0} = -p_0\varepsilon^2/2I_2 + \mathcal{O}(\varepsilon^3)$ and $\chi_2 = \chi_2^{(0)} + \mathcal{O}(\varepsilon^3)$. Proceeding, the effect of the perturbation at the third order in ε must be studied among the remaining $N-2$ degenerate states. By induction we thus have a whole hierarchy of roots, each corresponding to a different order in ε and determined by secular equations involving the corresponding perturbation operator that acts in the still degenerate subspace $V_n = (V_{i,j})_{n \leq i, j \leq N}$ expanded up to $\mathcal{O}(\varepsilon^n)$. It is clear that, at any given order of the perturbation theory, the resonances which are not anymore part of the degenerate subspace will have further corrections to their values. However we do not need to take them into consideration since we are only interested in the leading contributions to every resonance of the spectrum. In fact we can prove the

Proposition 4.1. The N roots of Eq. (18) can be approximated to order N in ε by $s_{1,0}, \dots, s_{N,0}$, where, for every $1 \leq n \leq N$, $s_{n,0}$ is the only root of order ε^n of the secular equation

$$\det[V_n(s)] = 0, \quad (33)$$

with leading contribution

$$s_{n,0} = -\frac{p_0\varepsilon^n}{2I_n} + \mathcal{O}(\varepsilon^{n+1}). \quad (34)$$

The corresponding right-eigenvector χ , Eq. (26), has coefficients c_n, \dots, c_N which are the solutions of the linear system

$$\sum_{k=n}^N V_{j,k}(s_{n,0}) c_k = 0, \quad j \geq n, \quad (35)$$

Left-eigenvectors $\tilde{\chi}$ have coefficients determined by

$$\sum_{j=n}^N V_{j,k}(s_{n,0}) c_j = 0, \quad k \geq n. \quad (36)$$

We will not discuss the states associated to $s_{n,m}$ ($m \neq 0$), which are exponentially decaying states and play a role only at the early stages of the dynamics.

From Eqs. (35) and (36) it is easy to show that to the leading order we have

$$\chi_n = \tilde{\chi}_n = \chi_n^{(0)} + \mathcal{O}(\varepsilon^n). \quad (37)$$

4.2. Algebraic Decay

According to Proposition 4.1, the resonances $s_{n,0}$ are $\mathcal{O}(\varepsilon^n)$ and therefore accumulate to $s=0$ as n becomes large, thus proving what we promised. Equation (17) together with Eq. (37) and the expression of the unperturbed eigenvectors, Eq. (25), allow us to evaluate the leading contribution to A_j : $A_j = 2\mu^j + \mathcal{O}(\varepsilon)$, where we have substituted $l_j = l_0\mu^j$ and $l_0 = 1$.

Turning back to Eq. (4), we have shown that the decay is algebraic as in Eq. (1) with

$$\delta = \frac{1}{\ln \varepsilon / \ln \mu - 1}. \quad (38)$$

We point out as a conclusion to this section that both parameters of the persistent hierarchical graph, ε and μ , are necessary to grant the algebraic decay of the survival probability. This point will be further discussed in the conclusions. In what follows we will derive further properties of the persistent hierarchical graphs, first classical and then quantum.

5. THERMODYNAMIC FORMALISM

For the real time process we consider, the free energy (usually referred to as topological pressure) per unit time is defined in analogy to continuous time processes where the stretching factors are here replaced by the inverses of the transition probabilities at the vertices of the graph.⁽³⁰⁾

$$\mathcal{F}(\beta) = \lim_{T \rightarrow \infty} \frac{1}{T} \ln \mathcal{L}_T(\beta), \quad (39)$$

where the dynamical partition function

$$\mathcal{Z}_T(\beta) = \sum_{\underline{b}_T} [P_{b_0 b_1} \cdots P_{b_{n-1} b_n}]^\beta \quad (40)$$

is the sum over all trajectories of time length T (or equivalently length $L = vT$) of their respective probabilities raised to the power β , with $\beta > 0$ playing the role of an inverse temperature. We note that the length of the trajectories cannot be measured sharply because of the continuous time nature of the system. Rather the sum in Eq. (40) should be understood as a sum over all trajectories whose lengths are within an interval $T \pm \Delta t$, where Δt is fixed. In the infinite T limit, the value of Δt is irrelevant.

Some properties of the free energy, are:⁽¹¹⁾ (i) \mathcal{F} is a monotonically decreasing function of β ; (ii) \mathcal{F} has a zero for some $\beta = d_H$, $0 < d_H < 1$ (the strict inequality being due to the open boundaries), where (iii) d_H is the fractal dimension of the repeller with respect to a properly defined metric space (in the sense that the space of trajectories is a continuum where trapped trajectories form a subset with fractal dimension); (iv) for hyperbolic systems of one degree of freedom, $-\mathcal{F}'(d_H)$ is the value of the positive Lyapunov exponent on the space of trapped trajectories; (v) $-\mathcal{F}(1)$ measures the rate of escape from the system; (vi) the difference between these last two quantities is the metric (Kolmogorov–Sinai) entropy on the repeller, $h_{KS} = \mathcal{F}(1) - \mathcal{F}'(d_H)$; and (vii) $\mathcal{F}(0) \equiv h_{TOP}$ is the topological entropy.

As argued in ref. 30, the free energy Eq. (39) can be obtained as the leading zero of the following zeta function $\zeta(s, \beta) = \det[1 - \mathbf{Q}_\beta(s)]$, where \mathbf{Q}_β is identical to the matrix \mathbf{Q} defined in Eq. (20), with the probabilities q_i and p_i now raised to the power β . Thus the free energy $\mathcal{F}(\beta)$ is the leading solution s of the expression $\prod_i \delta_i = 0$, where i takes values on the set of bonds and the δ_i are determined by the recurrence relation

$$\delta_i = 1 - q_i^\beta q_{i+1}^\beta e^{-2s_i} \left[1 + \left(\frac{p_i}{q_i} \right)^{2\beta} \left(\frac{1}{\delta_{i-1}} - 1 \right) \right], \quad (41)$$

$$\delta_1 = 1 - q_1^\beta q_2^\beta e^{-2s_1}. \quad (42)$$

We prove the following asymptotic behaviors :

Proposition 5.1. In the limit of large β , the free energy \mathcal{F} is linear in β with a coefficient exponentially small with respect to the number of bonds in the system, N ,

$$\lim_{\beta \rightarrow \infty} \mathcal{F}(\beta) = -\beta \frac{1 + \varepsilon}{2} \left(\frac{\varepsilon}{\mu} \right)^N. \quad (43)$$

The proof of this result follows by considering the probability of a particle bouncing off a given bond n for a time T . Let $W_T(n)$ be this probability. We have

$$\begin{aligned} W_T(n) &= [q_n q_{n+1}]^{T/2\mu^n}, \\ &= \left[1 - \frac{1+\varepsilon}{2} \left(\frac{\varepsilon}{\mu}\right)^n + O\left(\frac{\varepsilon^2}{\mu}\right)^n \right]^T. \end{aligned} \quad (44)$$

Thus the ratio

$$\frac{W_T(n)}{W_T(n-1)} = \left[1 + \frac{1+\varepsilon}{2} \left(1 - \frac{\varepsilon}{\mu}\right) \left(\frac{\varepsilon}{\mu}\right)^{n-1} + \dots \right]^T > 1 \quad (45)$$

is larger than 1, which implies that, as $\beta \rightarrow \infty$, the free energy is dominated by particles bouncing off the last bond, i.e., $F(\beta) \approx \lim_T (1/T) \ln[W_T(N)^\beta]$. Equation (43) follows.

Proposition 5.2. When β tends to zero, the free energy \mathcal{F} has a limit independent of ε , given by $\lim_{\beta \rightarrow 0} \mathcal{F}(\beta) \propto \frac{1}{\mu^N} [1 + O(\mu)]$. Thus in the limit of large number of bonds N , the free energy has a singular limit, $\lim_{N \rightarrow \infty} \mathcal{F}(0) = \infty$.

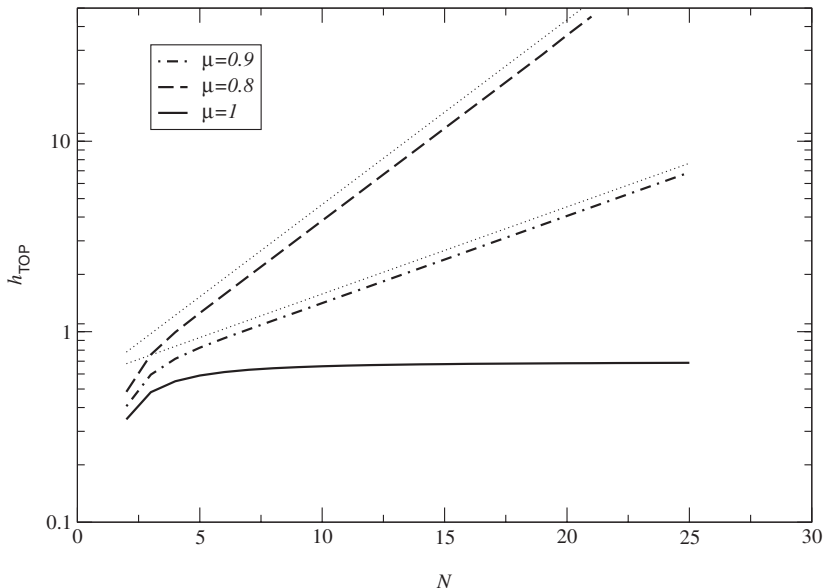


Fig. 4. Topological entropy vs. N for three different values of μ : $\mu = 1$ (solid line), $9/10$ (dot-dashed line) and $8/10$ (dashed line). The two dotted curves are proportional to $1/\mu^N$.

This holds since the rate of creation of new trajectories per collision is the same at every site, while the rate of collision per unit time increases exponentially as the particles go deeper into the lattice. Hence the topological entropy is overwhelmingly dominated by particles bouncing off the right-most bond. In particular, the reason for its diverging with $N \rightarrow \infty$ is due to the existence of trajectories undergoing an infinite number of collisions in a finite time, e.g., the trajectory ever moving to the right. Numerical evidence for Proposition 5.2 is shown in Fig. 4.

We close this section with the observation that, in the infinite system limit, we expect the free energy to have a phase transition at the value $\beta = 1$. This should result from the asymptotic behaviors of the free energy discussed in Propositions 5.1 and 5.2. In the limit $N \rightarrow \infty$, by Proposition 5.1, the free energy is zero for every $\beta > 1$ since it is zero at $\beta \rightarrow \infty$. On the other hand, by Proposition 5.2, it diverges as $\beta \rightarrow 0$, and thus must decrease steeply for $0 < \beta < 1$. We thus infer that matching the two curves at $\beta = 1$ results in a discontinuity of one of the derivatives of \mathcal{F} .

6. THE QUANTUM HIERARCHICAL GRAPH

In this section we wish to explore the possibility of having a scaling relation for the widths of the resonances, as was suggested in ref. 16. Numerical analysis of the time evolution of quantum systems as considered in refs. 27 and 36 is possible for a finite system, but goes beyond our scope. Thus we consider a quantum system whose classical limit is the one defined in Section 2.2. The quantum system is a linear chain with transition and reflection *probability amplitudes*

$$\left\{ \begin{array}{l} \sigma_{(n+1, +), (n, +)} = \sqrt{p_{n+1}}, \\ \sigma_{(n, -), (n, +)} = i \sqrt{q_{n+1}}, \\ \sigma_{(n-1, -), (n, -)} = \sqrt{p_n}, \\ \sigma_{(n, +), (n, -)} = i \sqrt{q_n}, \end{array} \right. \quad (46)$$

with p_n and q_n defined as in Eq. (7). $\sigma_{bb'} = 0$ for all other possibilities. It is clear that at each vertex the scattering matrix is unitary and therefore the quantum problem is well defined. Moreover we have that $P_{bb'} = |\sigma_{bb'}|^2$ which shows⁽²⁷⁾ that the classical limit of this quantum problem is indeed given by Eqs. (5) and (6).

The time evolution of a wave packet in an open system is controlled by the scattering resonances defined in the complex plane of wavenumbers k as the poles of the scattering matrix. For a quantum system, denoting

the wavefunction by $\psi(x_b, t)$, we can write the survival probability as: $P_{QM}(t) = \sum_b \int dx_b |\psi(x_b, t)|^2$. Letting $\psi(x_b, t) = \sum_r c_r(x_b) e^{-iE_r t}$, where $c_r(x_b)$ are determined by eigenstates of the evolution operator with complex eigenvalues E_r , we can rewrite the survival probability as follows :

$$P_{QM}(t) = \sum_{r,r'} c_r c_{r'} e^{i(\epsilon_r - \epsilon_{r'})t} e^{-(\Gamma_r + \Gamma_{r'})t/2}, \tag{47}$$

where we have used the decomposition $E_r = k_r^2 = \epsilon_r - i\Gamma_r/2$.

Since for short times the quantum evolution follows the classical one, it is interesting to study the distribution of scattering resonances in hierarchical graphs and look for manifestations of the algebraic decay in a quantum spectrum. Hufnagel *et al.*⁽¹⁶⁾ showed, in the framework of a quantum version of the chain model, that the distribution p of the width $\Gamma = -4 \operatorname{Re} k \operatorname{Im} k$ of the quantum scattering resonances k satisfies $p(\Gamma) \sim 1/\Gamma$, $\Gamma \ll 1$. Moreover, using an argument based on perturbation theory, they argued that the imaginary parts of the quantum scattering resonances satisfy a scaling relation.

Given a scaling relation for the resonance widths, $\Gamma_i = f^i$, the widths distribution follows:

$$p(\Gamma) = \sum_i \delta(\Gamma_i - \Gamma) \approx \int \delta(f^x - \Gamma) dx \sim \frac{1}{\Gamma} \tag{48}$$

This distribution has been associated to peaks that decorate fractal conductance fluctuations observed in energy scales larger than the mean level spacing. But since the width and height of the peaks in the conductance are determined by the imaginary part of the scattering resonances, the scaling behavior of the resonance widths is also contributing to the self similar, i.e., fractal, shape of the conductance.

The scattering resonances are the zeros of the zeta function $\det[1 - R(k)]$, with the matrix $R(k)$ obtained by replacing s by ik and $P_{bb'}$ by $\sigma_{bb'}$ in Eq. (20). As for the classical resonances, we can develop a perturbative approach in order to determine the quantum resonances and the corresponding eigenstates, $R(k) \phi = \phi$.

As opposed to the classical case, the zeroth order resonances are generally non-degenerate. Indeed a straightforward calculation of $\det[1 - R(k)]$ with $\varepsilon = 0$ yields the roots

$$k_{n,p}^{(0)} = \frac{(2p+1)\pi}{2l_n}, \quad p \in \mathbb{Z}. \tag{49}$$

Similarly to Eq. (25), the eigenvector corresponding to $k_{n,p}$ is given by

$$\phi_{n,p} = (0 \quad \cdots \quad 0 \quad \overbrace{1 \quad (-1)^p}^{2n-1 \quad 2n} \quad 0 \quad \cdots \quad 0). \quad (50)$$

Unless $\mu = 1$, the zeroth order quantum resonances are all isolated, whereas, for $\mu = 1$, $k_{n,p}^{(0)} = (2p+1)\pi/2$ is independent of n , so that, for every different p , the resonances have an N th order degeneracy. We consider the two different cases separately.

6.1. Non-Hierarchical Graph: $\mu = 1$

For $\mu = 1$, the situation is similar to Section 4. We can proceed by analogy and show the following

Proposition 6.1. For equally inter spaced scatterers, i.e., $\mu = 1$, the quantum resonances are given by

$$k_{n,p} = \frac{(2p+1)\pi}{2} - i \frac{P_0 \varepsilon^n}{4} + \mathcal{O}(\varepsilon^{n+1}), \quad p \in \mathbb{Z} \quad (\mu = 1). \quad (51)$$

Thus, for every integer p , the $k_{n,p}$ satisfy a scaling law and we have an accumulation point at $(2p+1)\pi/2$. Since the inverse of the lifetime is $\Gamma = -4 \operatorname{Re} k \operatorname{Im} k$ and $v = 2 \operatorname{Re} k$ is identified with the speed of the particle we have that $\Gamma_{n,p} = v \frac{P_0}{2} \varepsilon^j = s_j$.

This result shows that asymptotically the classical and quantum lifetimes of the resonances with longest lifetime coincide in the graph with evenly inter spaced scatterers ($\mu = 1$). This is in opposition to fully chaotic graphs where the strict inequality is satisfied $\gamma > \Gamma_{\min}$.⁽³⁷⁾ However there is no algebraic decay in this case.

6.2. Hierarchical Graph: $\mu \neq 1$

The case $\mu \neq 1$ is trickier. Indeed, one expects that the lowest order correction to $k_{n,p}$ is $\mathcal{O}(\varepsilon^n)$, but it can only be determined in the perturbation theory provided we know the $n-1$ th order correction to the roots $k_{n',p'}$ with $n' < n$, as well as the corresponding eigenvectors. In the remaining of this section, we will outline the derivation of the first order resonances and their eigenvectors and present in Table I the results of a computation of $k_{n,p}$ to fourth order of perturbation theory.

Table I. Quantum Resonances up to Fourth Order in ε . The Zeroth Order Resonance $k_{n,p}^{(0)}$ Is Here Written Modulo $2\pi/\mu^n$. Notice that the Second Order Correction to $k_{2,p}$ Is Purely Real. The Same Holds for the Third and Fourth Order Corrections to $k_{3,p}$. This Suggests that the Imaginary Parts of $k_{n,p}$ Are $\mathcal{O}(\varepsilon^{2n-1})$

n	p	$\mathcal{O}(\varepsilon^0)$	$\mathcal{O}(\varepsilon^1)$	$\mathcal{O}(\varepsilon^2)$	$\mathcal{O}(\varepsilon^3)$
1	1	$\frac{\pi}{2\mu}$	$-\frac{ip_0}{4\mu}$	$-\frac{ip_0[2-2e^{i\pi\mu}+p_0+e^{i\pi\mu}p_0]}{8[1+e^{i\pi\mu}]\mu}$	$-i\frac{[1+e^{i\pi\mu}]^2p_0^3-3e^{i\pi\mu}p_0^2\mu}{12[1+e^{i\pi\mu}]^2\mu}$
1	0	$-\frac{\pi}{2\mu}$	$-\frac{ip_0}{4\mu}$	$-\frac{ip_0[-2+2e^{i\pi\mu}+p_0+e^{i\pi\mu}p_0]}{8[1+e^{i\pi\mu}]\mu}$	$-i\frac{[1+e^{i\pi\mu}]^2p_0^3-3e^{i\pi\mu}p_0^2\mu}{12[1+e^{i\pi\mu}]^2\mu}$
2	1	$\frac{\pi}{2\mu^2}$	0	$i\frac{[-1+e^{i\pi/\mu}]p_0}{4[1+e^{i\pi\mu}]\mu^2}$	$-i\frac{-[1+e^{i\pi/\mu}]^2[-1+e^{i\pi\mu}]p_0+e^{i\pi/\mu}[1+e^{i\pi\mu}]p_0^2}{4[1+e^{i\pi/\mu}]^2[1+e^{i\pi\mu}]\mu^2}$
2	0	$-\frac{\pi}{2\mu^2}$	0	$-i\frac{[-1+e^{i\pi/\mu}]p_0}{4[1+e^{i\pi\mu}]\mu^2}$	$-i\frac{[1+e^{i\pi/\mu}]^2[-1+e^{i\pi\mu}]p_0+e^{i\pi/\mu}[1+e^{i\pi\mu}]p_0^2}{4[1+e^{i\pi/\mu}]^2[1+e^{i\pi\mu}]\mu^2}$
3	1	$\frac{\pi}{2\mu^3}$	0	0	$i\frac{[-1+e^{i\pi/\mu}]p_0}{4[1+e^{i\pi\mu}]\mu^3}$
3	0	$-\frac{\pi}{2\mu^3}$	0	0	$-i\frac{[-1+e^{i\pi/\mu}]p_0}{4[1+e^{i\pi\mu}]\mu^3}$
4	1	$\frac{\pi}{2\mu^4}$	0	0	0
4	0	$-\frac{\pi}{2\mu^4}$	0	0	0
n	p	$\mathcal{O}(\varepsilon^4)$			
1	1	$-i\frac{[1+e^{i\pi\mu}]^3p_0^4-2[-1+e^{i\pi\mu}]p_0^2[1+e^{2i\pi\mu}-2e^{i\pi\mu}(-1+\mu)]+e^{i\pi\mu}p_0^3[-2+e^{i\pi\mu}(-2+\mu)-\mu]\mu}{16[1+e^{i\pi\mu}]^3\mu}$			
1	0	$-i\frac{[1+e^{i\pi\mu}]^3p_0^4+2[-1+e^{i\pi\mu}]p_0^2[1+e^{2i\pi\mu}-2e^{i\pi\mu}(-1+\mu)]-e^{i\pi\mu}p_0^3[2+e^{i\pi\mu}(2+\mu)-\mu]\mu}{16[1+e^{i\pi\mu}]^3\mu}$			
2	1	$i\frac{p_0^2[-2\mu+(4-2\mu-p_0\mu)e^{i\pi/\mu}-(4-p_0\mu+3p_0\mu)e^{2i\pi/\mu}+2\mu e^{3i\pi\mu}]}{16[1+e^{i\pi/\mu}]^3\mu^3}$			
2	0	$-i\frac{p_0^2[-2\mu+(4-2\mu+3p_0\mu)e^{i\pi/\mu}-(4-p_0\mu-p_0\mu)e^{2i\pi/\mu}+2\mu e^{3i\pi\mu}]}{16[1+e^{i\pi/\mu}]^3\mu^3}$			
3	1	$i\frac{[-1+e^{i\pi\mu}]p_0}{4[1+e^{i\pi\mu}]\mu^3}$			
3	0	$-i\frac{[-1+e^{i\pi\mu}]p_0}{4[1+e^{i\pi\mu}]\mu^3}$			
4	1	$i\frac{[-1+e^{i\pi/\mu}]p_0}{4[1+e^{i\pi\mu}]\mu^4}$			
4	0	$-i\frac{[-1+e^{i\pi/\mu}]p_0}{4[1+e^{i\pi\mu}]\mu^4}$			

In order to find the solution of $\mathbf{R}(k_{n,p}) \phi_{n,p} = \phi_{n,p}$, we will write again $\mathbf{R}(k_{n,p}) = \mathbf{R}^{(0)}(k_{n,p}^{(0)}) + \delta\mathbf{R}(k_{n,p})$. Upon expanding the eigenvectors $\phi_{n,p}$ in terms of the basis spanned by the zeroth order eigenvectors $\phi_{n,0}^{(0)}$ and $\phi_{n,1}^{(0)}$, $\phi_{n,p} = \sum_{m=1}^N \sum_{q=0,1} c_{n,p,m,q} \phi_{m,q}^{(0)}$, we will make use of the property that $\phi_{m,q}^{(0)}$ is an eigenvector of $\mathbf{R}^{(0)}(k_{n,p}^{(0)})$, $\mathbf{R}^{(0)}(k_{n,p}^{(0)}) \phi_{m,q}^{(0)} = \Lambda_{n,p,m,q} \phi_{m,q}^{(0)}$, with eigenvalue $\Lambda_{n,p,m,q} = (-1)^q i \exp[(-1)^{p+1} i\pi\mu^{m-n}/2]$. The first order correction to $k_{n,p}^{(0)}$ is the solution $k_{n,p}^{(1)}$ of the equation $\phi_{n,p}^{(0)\text{T}} \delta\mathbf{R}(k_{n,p}^{(0)} + \varepsilon k_{n,p}^{(1)}) \phi_{n,p}^{(0)} = 0$, where $\delta\mathbf{R}$ must be expanded to first order in ε . The only non-zero first order corrections have $n = 1$, cf. Table I. The corresponding corrections to the zeroth order eigenvectors are given by

$$c_{n,p,m,q} = \frac{1}{\varepsilon} \frac{\phi_{m,q}^{(0)\text{T}} \delta\mathbf{R}(k_{n,p}^{(0)} + \varepsilon k_{n,p}^{(1)}) \phi_{n,p}^{(0)}}{1 - \Lambda_{n,p,m,q}}, \quad (m, q) \neq (n, p), \quad (52)$$

which are different from zero for $(m = 1, q = 1 - p)$ and $(m = 2, q = 0, 1)$. One can proceed to higher orders along these lines. The results for $k_{n,p}$ are presented in Table I up to fourth order. We note that our results suggest that the imaginary parts of the $k_{n,p}$ are $\mathcal{O}(\varepsilon^{2n-1})$. Given that the distribution of the real parts of the $k_{n,p}$ is rather uniform, this implies that the widths Γ scale identically to the imaginary parts of the scattering resonances. Hence Eq. (48) seems to hold for this example.

7. CONCLUSIONS

We have presented a simple model of an open hierarchical graph for which an analytical treatment of the algebraic decay of the survival probability is possible. The novelty of our approach lies on the successful application to the persistent hierarchical graph of a formalism originally developed in the framework of fully chaotic systems, where the survival probability decays exponentially.

For the classical system, the computation of the survival probability was done using the spectral decomposition of the evolution operator. We showed that the algebraic decay relies in an essential way on the scaling properties of both the Pollicott–Ruelle resonances and their amplitudes. Using a perturbative approach we argued that the resonance spectrum has an accumulation point at the value zero, which is characterized by a scaling property in terms of powers of the expansion parameter. The structure of the corresponding eigenstates with respect to the length scales of the system yields the scaling of the amplitudes.

This result must be contrasted to the observation of algebraic decay in the self-similar Markov chains.^(3,16) Although the exponents are identical,

the hierarchical graph is a dynamical process where randomness is involved only through the modelization of the collisions with scatterers, as opposed to self-similar Markov chains where transitions between states lack the spatial structure of our system. In the persistent hierarchical graph, the geometric role of the parameter μ is very clear, whereas in the self-similar Markov chains, μ represents an area which affects the transition probabilities between states.

As already pointed out in the introduction, the parameters ϵ and μ define a hierarchical dynamical trap,^(20, 21) in the sense that μ is the ratio between successive length scales and μ/ϵ the ratio between the corresponding staying times. Our result Eq. (38) is another instance of the relation of these parameters to the transport properties of the system, in this case the algebraic decay that characterizes the survival probability. It would be interesting to know what relation does this bear to the transport exponent of anomalous diffusion.

Other aspects of the properties of the classical persistent hierarchical graph were studied through the application of the thermodynamic formalism. We computed the free energy (or topological pressure) per unit time in terms of the leading zero of a zeta function defined in analogy to discrete time systems. Different asymptotic regimes were studied. In particular, the topological entropy, which is the infinite temperature limit ($\beta \rightarrow 0$) of the free energy, increases exponentially with the number of bonds in the graph. In the limit of large number of bonds, the low temperature ($\beta \gg 1$) free energy tends to zero exponentially with respect to the ratio $\epsilon/\mu < 1$. Moreover these results suggest that the free energy undergoes a phase transition at $\beta = 1$.

For the quantum system, we used methods similar to the classical case and conjectured that the widths of the quantum scattering resonances follow a scaling law, in agreement with the numerically observed width distribution.⁽¹⁶⁾ This argument was motivated by the computation of the resonances to the first few orders in perturbation theory. The limitation of this result, due to the complexity of the resolution of the quantum problem, illustrates the gap that separates the understandings of the classical and quantum approaches. The resolution of this question is open to future research by Bob Dorfman and others.

ACKNOWLEDGMENTS

This paper is dedicated to our friend, mentor and colleague Bob Dorfman, on the occasion of his 65th birthday. *Lechaim!* The authors are grateful to Vered Rom-Kedar and Uzy Smilansky for their helpful comments on the manuscript. We thank the Israeli Council for Higher

Education and the Feinberg postdoctoral fellowships program at the Weizmann Institute of Science for financial support. F.B. thanks the “Fundación Andes” and their program “inicio de carrera para jóvenes científicos” c-13760.

REFERENCES

1. B. V. Chirikov and D. L. Shepelyansky, Correlation properties of dynamical chaos in Hamiltonian systems, *Phys. D* **13**:395 (1984).
2. R. S. MacKay, J. D. Meiss, and I. C. Percival, Transport in Hamiltonian systems, *Phys. D* **13**:55 (1984).
3. J. D. Hanson, J. R. Cary, and J. D. Meiss, Algebraic decay in self-similar Markov chains, *J. Statist. Phys.* **39**:327 (1985).
4. J. D. Meiss and E. Ott, Markov tree model of intrinsic transport in Hamiltonian systems, *Phys. Rev. Lett.* **55**:2741 (1985).
5. J. D. Meiss and E. Ott, Markov tree model of transport in area-preserving maps, *Phys. D* **20**:387 (1986).
6. R. S. MacKay, J. D. Meiss, and I. C. Percival, Resonances in area-preserving maps, *Phys. D* **27**:1 (1987).
7. J. D. Meiss, Symplectic maps, variational principles, and transport, *Rev. Mod. Phys.* **64**:795 (1992).
8. M. Pollicott, On the rate of mixing of axiom A flows, *Invent. Math.* **81**:413 (1985). D. Ruelle, Resonances of chaotic dynamical systems, *Phys. Rev. Lett.* **56**:405 (1986); Locating resonances for Axiom A dynamical systems, *J. Statist. Phys.* **44**:281 (1986); Resonances for Axiom A flows, *J. Differential Geom.* **25**:99 (1987); One-dimensional Gibbs states and Axiom A diffeomorphisms, *J. Differential Geom.* **25**:117 (1987).
9. J. R. Dorfman, *An Introduction to Chaos in Non-Equilibrium Statistical Mechanics* (Cambridge University Press, Cambridge, UK, 1999).
10. P. Gaspard, *Chaos, Scattering and Statistical Mechanics* (Cambridge University Press, Cambridge, UK, 1998).
11. P. Gaspard and J. R. Dorfman, Chaotic scattering theory, thermodynamic formalism, and transport coefficients, *Phys. Rev. E* **52**:3525 (1995).
12. J. R. Dorfman and P. Gaspard, Chaotic scattering theory of transport and reaction-rate coefficients, *Phys. Rev. E* **51**, 28 (1995).
13. P. Gaspard and G. Nicolis, Transport properties, Lyapunov exponents, and entropy per unit time, *Phys. Rev. Lett.* **65**:1693 (1990).
14. J. Weber, F. Haake, and P. Šeba, Frobenius–Perron resonances for maps with a mixed phase space, *Phys. Rev. Lett.* **85**:3620 (2000).
15. M. Khodas, S. Fishman, and O. Agam, Relaxation to the invariant density for the kicked rotor, *Phys. Rev. E* **62**:4769 (2000).
16. L. Hufnagel, R. Ketzmerick, and M. Weiss, Conductance fluctuations of generic billiards: Fractal or isolated?, *Europhys Lett.* **54**:703 (2001).
17. G. A. van Velzen, *Lorentz Lattice Gases*, Ph.D. thesis (University of Utrecht, Utrecht, 1990).
18. J. R. Dorfman, M. H. Ernst, and D. Jacobs, Dynamical chaos in the Lorentz lattice gas, *J. Statist. Phys.* **81**:497 (1995).
19. P. Gaspard, Hydrodynamic modes as singular eigenstates of the Liouvillian dynamics: Deterministic diffusion, *Phys. Rev. E* **53**:4379 (1996).

20. G. M. Zaslavsky, *Physics of Chaos in Hamiltonian Systems* (Imperial College Press, London, 1998).
21. G. M. Zaslavsky, Chaotic dynamics and the origin of statistical laws, *Physics Today* 39 (August 1999).
22. R. Ketzmerick, Fractal conductance fluctuations in generic chaotic cavities, *Phys. Rev. B* 54:10841 (1996).
23. T. Kottos and U. Smilansky, Quantum chaos on graphs, *Phys. Rev. Lett.* 79:4794 (1997); Periodic orbit theory and spectral statistics for quantum graphs, *Ann. Physics* 274:76 (1999).
24. H. Schanz and U. Smilansky, Spectral statistics for quantum graphs: Periodic orbits and combinatorics, *Philos. Mag. B* 80:1999 (2000).
25. G. Berkolaiko and J. P. Keating, Two-point spectral correlations for star graphs, *J. Phys. A: Math. & Gen.* 32:7827 (1999).
26. F. Barra and P. Gaspard, On the level spacing distribution in quantum graphs, *J. Statist. Phys.* 101:283 (2000).
27. F. Barra and P. Gaspard, Transport and dynamics on open quantum graphs, *Phys. Rev. E* 65:016205 (2002).
28. T. Kottos and U. Smilansky, Chaotic scattering on graphs, *Phys. Rev. Lett.* 85:968 (2000).
29. H. Schanz and U. Smilansky, Periodic-orbit theory of Anderson localization on graphs, *Phys. Rev. Lett.* 84:1427 (2000).
30. F. Barra and P. Gaspard, Classical dynamics on graphs, *Phys. Rev. E* 63:66215 (2001).
31. B. Shapiro, Quantum conduction on a Cayley tree, *Phys. Rev. Lett.* 50:747 (1983).
32. G. Berkolaiko, *Quantum Star Graphs and Related Systems*, Ph.D. thesis (Bristol University, 2000).
33. K. Naimark, *Eigenvalue Behavior for the Equation-Lambda $u''=Vu''$* , Ph.D. thesis (Weizmann Institute of Science, 2000).
34. L. D. Landau and E. Lifshitz, *Quantum Mechanics*, 3rd Ed. (Pergamon Press, 1994).
35. P. Gaspard and F. Baras, Chaotic scattering and diffusion in the Lorentz gas, *Phys. Rev. E* 51:5332 (1995).
36. A. Jordan and M. Srednicki, *The Approach to Ergodicity in the Quantum Baker's Map*, Preprint nlin.CD/0108024.
37. P. Gaspard and S. A. Rice, Scattering from a classically chaotic repeller, *J. Chem. Phys.* 90:2225 (1989); Semi-classical quantization of the scattering from a classically chaotic repeller, 90:2242 (1989); Exact quantization of the scattering from a classically chaotic repeller, 90:2255 (1989); Erratum: "Scattering from a classically chaotic repeller," 91:3279 (1989); Erratum: "Semi-classical quantization of the scattering from a classically chaotic repeller," 91:3279 (1989) Erratum: "Exact quantization of the scattering from a classically chaotic repeller," 91:3280 (1989).